Functional, Uniform, and Macroporous Latex Particles: Preparation, Electron Microscopic Characterization, and Nonspecific Protein Adsorption Properties

T. ÇAMLI,[1] M. TUNCEL,[2] S. ŞENEL,[1] A. TUNCEL[3]

[1] Chemistry Department, Hacettepe University, 06532, Ankara, Turkey

[2] Anatomy Department, Hacettepe University, 06532, Ankara, Turkey

[3] Chemical Engineering Department, Hacettepe University, 06532, Ankara, Turkey

Received 5 January 2001; accepted 5 June 2001

ABSTRACT: A series of uniform, macroporous particles with different surface chemistries were prepared with different acrylic comonomers [methyl methacrylate (MMA), butyl methacrylate (BMA), epoxypropyl methacrylate (EPMA), 2-hydroxyethyl methacrylate (HEMA), and methacrylic acid (MAA)] with styrene–divinylbenzene (S–DVB) in a multistep seeded polymerization. In the synthesis, uniform polystyrene seed particles 6.2 μm in size were swollen first with a low molecular weight organic agent and then with a monomer phase including an S–DVB mixture and a relatively polar acrylic monomer. Final macroporous particles approximately 10 μm in size were obtained by the repolymerization of the monomer phase in the swollen seed particles. Surface and bulk morphologies were investigated with scanning and transmission electron microscopy, respectively. Although highly porous particles could be achieved with relatively hydrophobic monomers such as styrene, BMA, MMA, and EPMA, the use of hydrophilic monomers such as HEMA and MAA led to the synthesis of uniform particles with lower macroporosity. A comparison of Fourier transform infrared and Fourier transform infrared/diffuse reflectance spectroscopy spectra indicated that the concentration of polar acrylic monomer on the surface was higher than in the bulk structure. The nonspecific protein adsorption behavior of uniform, macroporous particles was investigated with albumin as a model protein. The highest nonspecific albumin adsorption was observed with plain poly(styrene-*co*-divinylbenzene) [poly(S–DVB)] particles. The particles produced with MMA and EPMA also exhibited albumin adsorption capacities very close to that of plain poly(S–DVB). Reasonably low nonspecific albumin adsorption was observed with the particles produced in the presence of MAA, HEMA, and BMA. Poly(S–DVB) particles functionalized with poly(vinyl alcohol) provided nearly zero nonspecific albumin adsorption. For nonspecific albumin binding onto the particles via a physical adsorption mechanism, desorption ratios higher than 80% could be achieved. The desorption ratio with the EPMA-carrying particles was only 5% because the albumin adsorption onto EPMA-carrying particles occurred predominantly with covalent-bond formation. J Appl Polym Sci 84: 414–429, 2002; DOI 10.1002/app.10412

Key words: emulsion polymerization; dispersion polymerization; uniform latex particles; porous particles; chromatographic packing; protein adsorption; albumin; bioaffinity chromatography

Correspondence to: A. Tuncel (atuncel@hacettepe.edu.tr).

INTRODUCTION

Macroporous latex particles 5–20 μm in size have been widely used as column-filling materials (i.e., stationary phases) in gel permeation chromatography (GPC) applications aiming at the qualitative or quantitative determination of different biochemicals. Most of the currently available macroporous particles used as column materials in GPC have been manufactured in the polydisperse form. Since the 1990s, uniform, macroporous particles have been promoted as new-generation column materials possessing significant advantages over conventional polydisperse particles.[1–4] A more regular flow regime in the column, lower column back-pressure, and chromatograms with higher resolutions are the known advantages of these new materials.[1–4]

Uniform, macroporous particles have usually been obtained with seeded polymerization techniques.[1–13] Ugelstad and coworkers[2,5,6] developed a two-step microsuspension method to produce compact or macroporous particles of predetermined size in a range of 1–20 μm. El-Aasser and coworkers[7,8] achieved the preparation of monodisperse macroporous polymer particles 10 μm in diameter via seeded emulsion polymerization. In their studies, a linear polymer [polystyrene (PS) seed] or a mixture of a linear polymer and a solvent or nonsolvent were tried as inert diluents to achieve macroporous structures with pore diameters of approximately 1000 Å and specific surface areas up to 250 m^2/g.[7,8] Frechet and coworkers[1,3,4] developed a multistage seeded polymerization for the synthesis of uniformly sized porous poly(styrene-*co*-divinylbenzene) [poly(S–DVB)] beads 7.4 μm in size. They also examined the chromatographic performance of the produced beads in size exclusion chromatography with different proteins of reasonably close molecular weights.[3] A dynamic swelling method was proposed by Okubo and Nakagawa[14] for the synthesis of highly crosslinked large, uniform latex particles. A new method, the Shirasu porous glass emulsification technique, was also introduced for the preparation of functional, uniform particles with diameters of 2.5–60 μm.[15–17]

Although production methods and formation mechanisms of uniform, macroporous particles have been extensively investigated, limited attention has been paid to the chemical modification of these particles. Most of the surface modification methods were developed for uniform latex particles produced by emulsion or dispersion polymerization processes in the size range of 0.1–2.0 μm.[18–35] Nonspecific protein adsorption behaviors of chemically modified latex particles in submicrometer or micrometer ranges have been extensively investigated.[18–27] Recently, thermosensitive polymeric latices have been tried as a novel class of sorbents in protein adsorption studies aiming to control the extent of nonspecific protein adsorption onto the polymeric surface by adjusting the medium temperature.[36–38] Similar thermosensitive particles in submicrometer ranges were used as support materials for the immobilization of different enzymes.[39,40] Latex particles in the submicrometer range were also tested as support materials for the immobilization of oligonucleotides, DNA fragments, and antibodies for diagnostic purposes.[41–46]

The hydrophilicity and surface chemistry of uniform, macroporous particles are important in GPC applications involving the detection or quantitative analysis of biomolecules such as proteins, glycoproteins, and nucleic acids. The surface chemistry is the most important factor for controlling the nonspecific adsorption behavior of biological agents onto the column materials. Today, most uniform, macroporous particles are produced in the form of styrene–divinylbenzene (S–DVB) copolymers.[1–13] The modification of these particles by the introduction of functional groups onto their surfaces allows either the regulation of surface hydrophobicity or the attachment of ligands for the synthesis of stationary phases with specific recognition abilities for different biomolecules.

Our recent studies were mainly focused on the production and surface modification of uniform, macroporous particles 5–20 μm in size and the interaction of these particles, with their different surface chemistries, with proteins.[10–13] Poly(vinyl alcohol) (PVA)-carrying uniform, macroporous particles, exhibiting no nonspecific protein adsorption, were derivatized by an albumin-specific ligand (i.e., Cibacron Blue F3G-A) for the synthesis of an albumin-specific stationary phase with a potential use in GPC.[12] In the development of a protein-specific sorbent, the definition of the nonspecific adsorption behavior of the base material is essential. For this reason, we investigated the nonspecific protein adsorption behavior of a series of uniform, macroporous particles prepared with different surface chemistries as potential stationary phases in GPC applications. Here we report on the production method, surface and

bulk characteristics, and albumin adsorption behaviors of these particles.

EXPERIMENTAL

Materials

Styrene (S; Yarpet AS, Kocaeli, Turkey) was distilled *in vacuo* and stored in a refrigerator until use. Divinylbenzene (DVB; including 55% *para*- and *meta*-DVB isomers; Aldrich Chemical Co., Milwaukee, WI) was extracted with a 5% (w/w) aqueous NaOH solution for removal of the inhibitor. Methacrylic acid (MAA; Merck, AG, Darmstad, Germany), 2-hydroxyethyl methacrylate (HEMA, Sigma Chemical Co., St. Louis, MO), methyl methacrylate (MMA; Aldrich Chemical), butyl methacrylate (BMA; Aldrich Chemical), and epoxypropyl methacrylate (EPMA, Aldrich Chemical) were selected as acrylic comonomers. MMA was extracted with a 5% (w/w) aqueous NaOH solution before use, whereas the others were used as received. Sodium lauryl sulfate (Sigma Chemical) was the emulsifier in the preparation of aqueous emulsion media for the swelling of seed particles. Dibutyl phthalate (Polisan AS, Kocaeli, Turkey) was used as the diluent. An oil-soluble initiator, benzoyl peroxide (BPO; Aldrich Chemical), was used for the repolymerization of the monomer phase in the swollen seed particles. Bovine serum albumin (BSA; Fraction V, Sigma Chemical) was used in the adsorption experiments. Polymerizations and albumin adsorption experiments were performed with distilled and deionized (DDI) water.

Preparation of Uniform PS Seed Particles

The seed latex particles were obtained by dispersion polymerization. Typically, S (5 mL) was dissolved in a homogeneous mixture of ethanol (18 mL; Merck AG) and 2-methoxyethanol (high performance liquid chromatography (HPLC) grade, 12 mL; Aldrich Chemical) including poly(vinylpyrollidone) (PVP; PVP-40, average molecular weight = 40.000, intrinsic viscosity = 29–32, 0.525 g; Sigma Chemical) as the steric stabilizer. The initiator, freshly crystallized 2,2′-azobisizobutyronitrile (0.11 g; BDH Chemicals Ltd., Poole, England) was dissolved in the resulting homogeneous mixture. The sealed Pyrex polymerization reactor was placed in a shaking water bath equipped with a heater and a temperature-control system. The polymerization was conducted at 70°C for 24 h at a 150-cpm shaking rate. The product was 6.2-μm PS latex particles. The latex particles were extensively washed with DDI water with a centrifugation–decantation procedure. The molecular weight of the seed latex was determined in an HPLC system (Waters, Milford, MA) with methylene chloride as the eluent in an Ultrastyragel column operated at ambient temperature with PS standards.

Synthesis of Large Uniform Latex Particles

The multistep seeded polymerization used in our study was developed according to the principles of the polymerization method proposed by Wang et al.[3] Large uniform latex particles were obtained with a two-step seeded polymerization procedure. By following this method, we obtained uniform particles of plain poly(S–DVB), poly(vinyl alcohol)-carrying poly(styrene-*co*-divinylbenzene) [PVA–poly(S–DVB)], poly(styrene–methyl methacrylate–divinylbenzene) [poly(S–MMA–DVB)], poly(styrene–butyl methacrylate–divinylbenzene) [poly(S–BMA–DVB)], poly(styrene–epoxypropyl methacrylate–divinylbenzene) [poly(S–EPMA–DVB)], poly(styrene–methacrylic acid–divinylbenzene) [poly(S–MAA–DVB)], and poly(styrene–hydroxyethyl methacrylate–divinylbenzene) [poly(S–HEMA–DVB)].

In a typical synthesis, dibutylphthalate (0.35 mL) was emulsified in 25 mL of an aqueous medium including 0.25% (w/w) sodium dodecyl sulfate (SDS) as the emulsifier. For the emulsification, a mixture of dibutyl phthalate (DBP) and aqueous SDS was sonicated for 30 min in an ultrasonic water bath (Bransonic 200, Orange, VA). An aqueous dispersion of PS seed particles (ca. 4.0 mL) including 0.35 g of PS seed particles was added to the DBP emulsion. The resulting dispersion was stirred magnetically (400 rpm) at room temperature for 24 h for the complete absorption of DBP by the PS seed particles. In the next step, a monomer phase, consisting of S (0.4 mL), DVB (0.8 mL), an acrylic monomer (i.e., MMA, BMA, EPMA, HEMA, or MAA; 0.4 mL), and BPO (60 mg), was emulsified in 25 mL of an aqueous medium including 0.25% (w/w) SDS by sonication for 5 min. The monomer emulsion was then mixed with the aqueous dispersion of DBP-swollen seed particles. The resulting emulsion was stirred at room temperature for 8 h at 400 rpm for the absorption of the monomer phase by the DBP-swollen seed particles. At the end of this

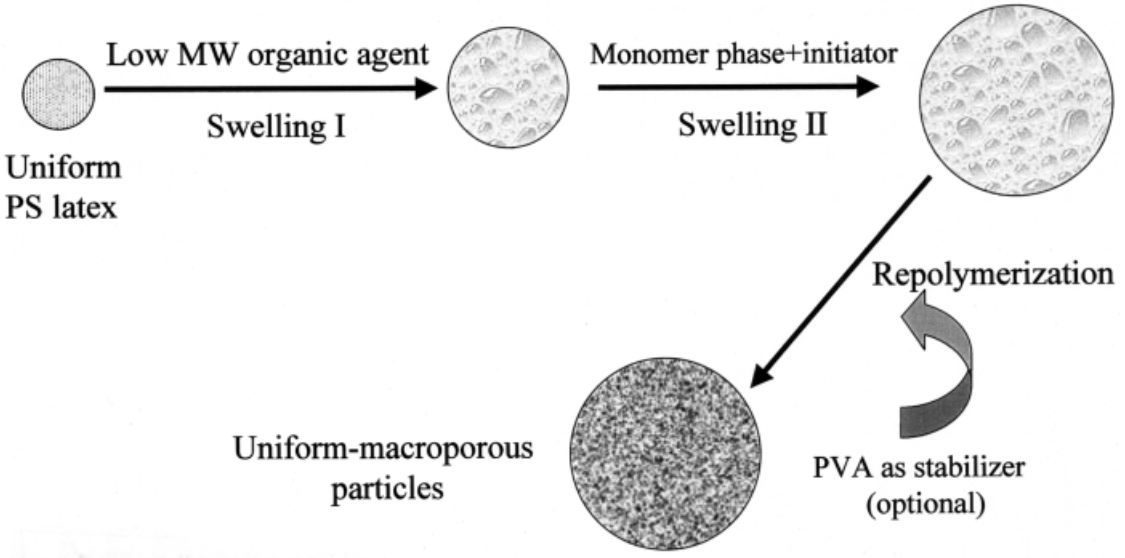

Figure 1 Schematic representation of the seeded polymerization used for the preparation of the macroporous particles.

period, the emulsion was purged with bubbling nitrogen for 5 min. Repolymerization of the monomer phase in the swollen seed particles was conducted at 70°C for 24 h at a 120-cpm shaking rate. Repolymerization provided macroporous particles with different surface chemistries. In some preparations, latex particles approximately 1 μm in size were obtained as a byproduct together with the large uniform fraction. These small particles were discarded with a successive centrifugation–decantation procedure, and the large macroporous fraction was isolated. For the synthesis of PVA-carrying poly(S–DVB) particles, PVA was used as a steric stabilizer in the repolymerization step. For other particle types, the repolymerizations were performed without PVA. A schematic representation of the seeded polymerization used for the synthesis of the uniform, macroporous particles is given in Figure 1. The final particles were washed with tetrahydrofuran and ethanol extensively for removal of the diluent and the linear polymer with successive centrifugation and decantation steps. Then, the particles were washed with water and redispersed via shaking in DDI water.

Characterization of the Uniform Latex Particles

The average size and size distribution of particles were determined with scanning electron microscopy (SEM; JEOL JEM 1200EX, Tokyo, Japan). An aqueous dispersion of cleaned latex particles (ca. 0.1 mL) was spread onto a copper disk, and water was evaporated. Dried particles were coated with a thin layer of gold (ca. 100 Å) *in vacuo*. The specimens were examined and photographed with SEM (JEOL JEM 1200 EX). The magnification was set to 1000× in the SEM photographs taken for the determination of the average size and coefficient of variation (CV). For each particle type, two different SEM photographs were taken from different fields. The photographs were printed at 14 cm × 10 cm, and all beads in the photographs were measured and counted for the determination of size distribution properties. Through the evaluation of the SEM photographs, the number-average diameter (D_n) of the particles was calculated according to eq. (1), where N_i is the number of particles with diameter D_i (μm):

$$D_n = \sum N_i D_i / \sum N_i \quad (1)$$

The weight-average diameter (D_w) was calculated with eq. (2):

$$D_w = \sum N_i D^4 / \sum N_i D_i^3 \quad (2)$$

The CV was calculated as the ratio of the standard deviation (SD) to D_n according to eq. (3):

$$\text{CV}\ (\%) = (SD/D_n) \times 100 \quad (3)$$

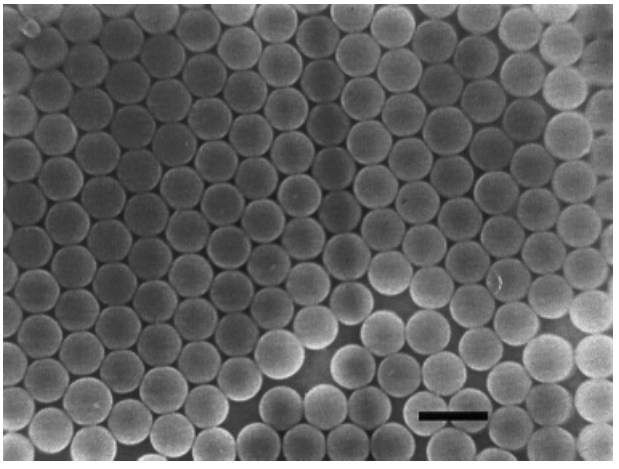

Figure 2 Typical SEM micrograph of the PS seed particles (the bar indicates 10 μm).

The surface morphology was evaluated by the SEM photographs taken at 4000× magnification. Transmission electron microscopy (TEM) was used for the examination of the bulk structure of the produced particles. For this purpose, dried particles (100–200 mg) were fixed in a 1% aqueous OsO_4 solution and dehydrated in a graded series of alcohols; they were then embedded in Araldit CY 212. Thin sections were cut serially (60–90 nm) with an Ultrathom (LKB, Tokyo, Japan), mounted on 100-mesh grids, and examined under a transmission electron microscope (JEOL JEM 1200 EX). Fourier transform infrared (FTIR) and Fourier transform infrared/diffuse reflectance spectroscopy (DRS) (FTIR–DRS) spectroscopy were used for examination of the bulk and surface chemistries of the particles. FTIR and FTIR–DRS spectra were obtained with KBr tablets and KBr powder, respectively. Before the related spectra were taken, the produced particles and KBr were first dried in a low vacuum at 40°C for 3 days and then over anhydrous $CaCl_2$ for 2 days. Mass-charge densities of the particles were determined by potentiometric titration performed with a 0.05*N* NaOH solution.

Nonspecific BSA Adsorption Experiments

In nonspecific BSA adsorption experiments performed in batch fashion, seven types of uniform latex particles with different surface chemistries [i.e., plain poly(S–DVB), PVA-carrying poly(S–DVB), poly(S–MMA–DVB), poly(S–BMA–DVB), poly(S–EPMA–DVB), poly(S–HEMA–DVB), and poly(S–MAA–DVB)] were used as sorbents. Typically, a certain amount of BSA was dissolved in a buffer solution (40 mL) at pH 5.0. A certain volume of suspension including 0.25 g of uniform particles was centrifuged, and the liquid part was decanted. Precipitated particles were redispersed in the BSA solution. Equilibrium adsorption experiments were conducted at 25°C for 2 h at a stirring rate of 200 rpm. Preliminary experiments indicated that equilibrium was established within 20–30 min in the adsorption process. Then, an equilibrium period of 2 h was used in the protein adsorption runs. At the end of this period, the suspension was centrifuged, and the particles were separated from the adsorption medium. Albumin adsorption capacities of uniform, macroporous particles were determined by the measurement of the initial and final BSA concentrations by the Biuret method. In the nonspecific adsorption experiments, the initial BSA concentration and pH of the adsorption medium were changed. For the investigation of the reversible desorption behavior, uniform particles were first loaded with BSA in a medium with a pH of 5.0 with an initial BSA concentration of 5 mg/mL at 25°C. After establishment of the adsorption equilibrium, the particles carrying different amounts of BSA were transferred into the desorption media, including 1.0*M* NaSCN at pH 8.0. The final BSA concentration in the desorption medium was determined by the Biuret method after a release period of 1 h at 25°C.

RESULTS AND DISCUSSION

Characterization of the Uniform, Macroporous Particles

A typical electron micrograph of PS particles used as the seed latex in the production of functionalized, macroporous particles is given in Figure 2. The properties of the seed latex are summarized in Table I. As seen here, seed particles with a D_n value of 6.2 μm could be achieved with a sufficiently narrow size distribution by the application of a single-stage polymerization.

Table I Properties of PS Seed Particles

D_n (μ)	CV (%)	M_n
6.2	2.64	5.8×10^3

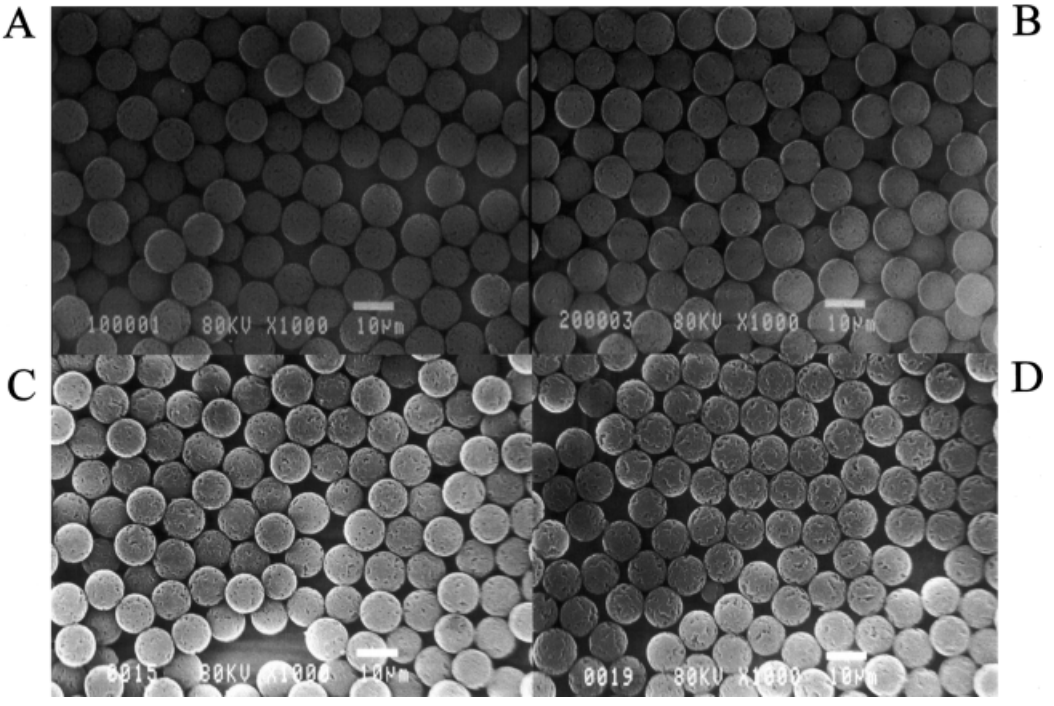

Figure 3 Electron micrographs showing the size and size distribution properties of the macroporous particles produced with relatively hydrophobic monomers in the repolymerization stage (for all photographs, the original magnification was 1000×): (A) poly(S–DVB) particles produced in the absence of PVA, (B) poly(S–DVB) particles produced in the presence of PVA, (C) poly(S–BMA–DVB) particles, and (D) poly(S–MMA–DVB) particles.

SEM photographs showing the size and size distribution of functionalized, macroporous particles obtained with relatively hydrophobic and hydrophilic comonomers in the seeded polymerization are given in Figures 3 and 4, respectively. The properties of the functionalized, macroporous particles are listed in Table II. For an idea of the polarity, Hansen solubility parameters of S and acrylic monomers are included in Table II. On the basis of the solubility parameter values, the most apolar structure was BMA. The polarity (i.e., the hydrophilicity) of the acrylic monomers increased with the increasing solubility parameter. Among the attempted structures, HEMA and MAA were infinitely soluble in water, whereas the others (i.e., EPMA, MMA, and BMA) had a limited solubility lower than 5 wt %. In all particle preparations, DVB and acrylic monomer feed concentrations in the repolymerized monomer mixture were fixed at 50 and 25% (v/v), respectively. As seen in Table II, the CV of produced particles was approximately 5% in most cases. These CVs indicated that all particle types were obtained with reasonably narrow size distributions. The repolymerization of the monomer mixture containing no acrylic monomer (i.e., S–DVB) provided a higher average size relative to the particles obtained in the presence of acrylic monomers. The highest mass-charge density was obtained with the plain poly(S–DVB) particles. The introduction of PVA or an acrylic monomer into the particle structure resulted in a decrease in the mass-charge density.

SEM photographs showing the detailed surface structures of the uniform, macroporous particles produced in the presence of S, BMA, and MMA are given in Figure 5. As seen here, particles with highly porous surfaces could be achieved when relatively hydrophobic monomers (i.e., S, BMA, and MMA) were used with DVB as the crosslinker. For the internal part, TEM photographs of OsO_4^{2-}-stained thin sections of the same particles are given in Figure 6. As seen here, all particle interiors were highly porous. An internal structure based on the homogeneous distribution of macropores in the whole cross section was observed for all particle types. A comparison of Figures 5 and 6 indicates that the average pore size on the particle surface was very close to that of

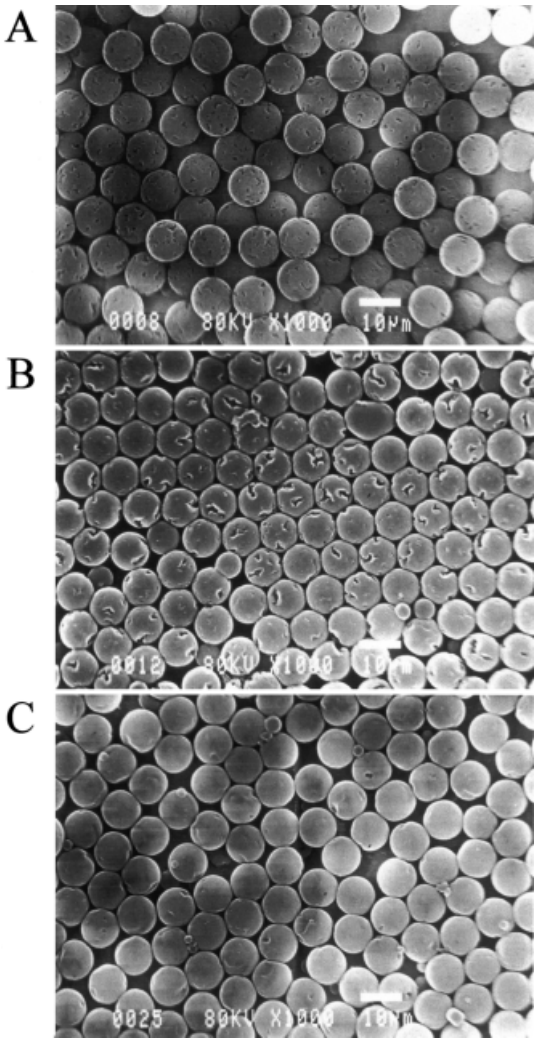

Figure 4 Electron micrographs showing the size and size distribution properties of the macroporous particles produced with relatively hydrophilic monomers in the repolymerization stage (for all photographs, the original magnification was 1000×): (A) poly(S–EPMA–DVB) particles, (B) poly(S–HEMA–DVB) particles, and (C) poly(S–MAA–DVB) particles.

the particle interior, and the pore size distributions of the particle surface and particle interior were similar for each particle type.

SEM photographs showing the surface structures of the particles produced with relatively polar acrylic monomers (i.e., EPMA, HEMA, and MAA) are given in Figure 7. As seen here, the particle surfaces obtained in the presence of polar acrylic monomers were reasonably different from those obtained with more hydrophobic monomers (Fig. 5). On the basis of the solubility parameters in Table II, EPMA should be considered the most apolar structure among the hydrophilic monomers tried. A relatively regular macroporous surface was only obtained for the particles produced in the presence of EPMA. However, the surface porosity of poly(S–EPMA–DVB) particles was lower than those of the particles produced with hydrophobic monomers such as S, BMA, and MMA (Fig. 5). However, HEMA and MAA were more polar relative to EPMA (Table II). As seen in Figure 7(B), there were craterlike and large macropores on the surface of poly(S–HEMA–DVB) particles. This view indicates that the macropore number density was lower on the surface of poly(S–HEMA–DVB) particles. The use of MAA in the repolymerized monomer mixture led to the synthesis of particles with a nonporous surface [Fig. 7(C)]. Note that both HEMA and MAA were infinitely soluble in water. These results confirmed that the surface porosity markedly decreased or disappeared in the presence of hydrophilic comonomers.

TEM photographs of OsO_4^{2-}-stained thin sections of the particles produced with EPMA, HEMA, and MAA are given in Figure 8. The bulk structure of poly(S–EPMA–DVB) particles was the most similar to those obtained with hydrophobic acrylic monomers (i.e., S, BMA, and MMA in Fig. 6). However, the bulk views of poly(S–HEMA–DVB) and poly(S–MAA–DVB) were reasonably different. Instead of a macroporous structure including homogeneously distributed pores of approximately equal sizes in the whole cross section, a porous structure including large voids was observed in the presence of HEMA and MAA. This structure was more characteristic for the particles produced with MAA [Fig. 8(C)]. Note that such a porous structure should have a significantly lower specific surface area and pore volume relative to those obtained in the presence of hydrophobic monomers.

FTIR and FTIR–DRS spectra of plain poly(S–DVB) and poly(S–DVB) particles produced with PVA as the stabilizer are given in Figure 9. As seen here, a reasonably characteristic FTIR spectrum was obtained for the plain poly(S–DVB) particles.[12,29] The weak band at 1740 cm^{-1} probably originated from the carbonyl groups of a covalently bound initiator used in the repolymerization (i.e., BPO). FTIR and FTIR–DRS spectra of plain poly(S–DVB) particles were reasonably similar. For poly(S–DVB) particles produced with PVA as the stabilizer, a clear hydroxyl band was detected at 3500 cm^{-1} in the FTIR–DRS spectrum. This band probably originated from the co-

Table II Properties of the Macroporous Particles

Particle Type	δ (cal/cm^3)$^{1/2}$	D_n (μm)	D_w (μm)	CV (%)	Q (mequiv/g) × 10^3
Plain poly(S–DVB)	9.3[a]	9.87	9.92	4.10	110.0
Poly(S–DVB) with PVA	—	10.03	10.11	5.84	18.9
Poly(S–BMA–DVB)	8.2[b]	9.53	9.58	4.23	68.7
Poly(S–MMA–DVB)	8.8[b]	9.43	9.50	5.97	13.7
Poly(S–EPMA–DVB)	9.5[c]	9.53	9.57	4.41	12.9
Poly(S–HEMA–DVB)	11.4[c]	9.42	9.52	7.20	79.4
Poly(S–MAA–DVB)	11.2[b]	9.46	9.52	5.37	21.1 (84.6)[d]

δ Hansen solubility parameter of of S and acrylic monomers; Q; mass-charge density based on acidic —OSO_3H groups of particles.

[a]The solubility parameter of S.

[b]The solubility parameters of BMA, MMA, and MAA were taken from ref. 47.

[c]The solubility parameters of EPMA and HEMA were calculated with the Hildebrand expression and molecular attraction constants in ref. 47, respectively.

[d]MAA content of poly(S–MAA–DVB) particles determined by potentiometric titration is given in the parenthesis as mg of MAA/g of particles.

valently bound or strongly entrapped PVA chains on the surface.[12] However, the hydroxyl band was very weak, in fact almost absent, in the FTIR spectrum, showing the bulk structure of the same particles. This indicated that PVA was predominantly located on the surface of poly(S–DVB) particles, and its bulk concentration in the whole particle structure was very low.

FTIR and FTIR–DRS spectra of poly(S–BMA–DVB) and poly(S–MMA–DVB) particles are given

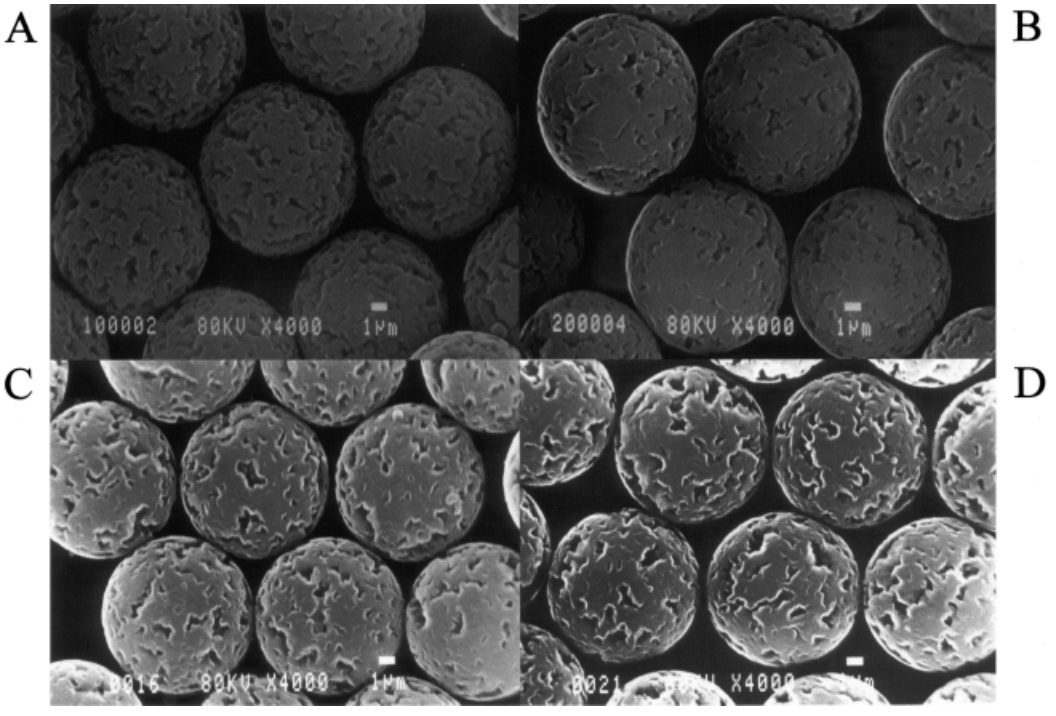

Figure 5 SEM photographs showing the detailed surface structures of the macroporous particles produced in the presence of relatively hydrophobic monomers in the repolymerization stage (for all photographs, the original magnification was 4000×): (A) poly(S–DVB) particles produced in the absence of PVA, (B) poly(S–DVB) particles produced in the presence of PVA, (C) poly(S–BMA–DVB) particles, and (D) poly(S–MMA–DVB) particles.

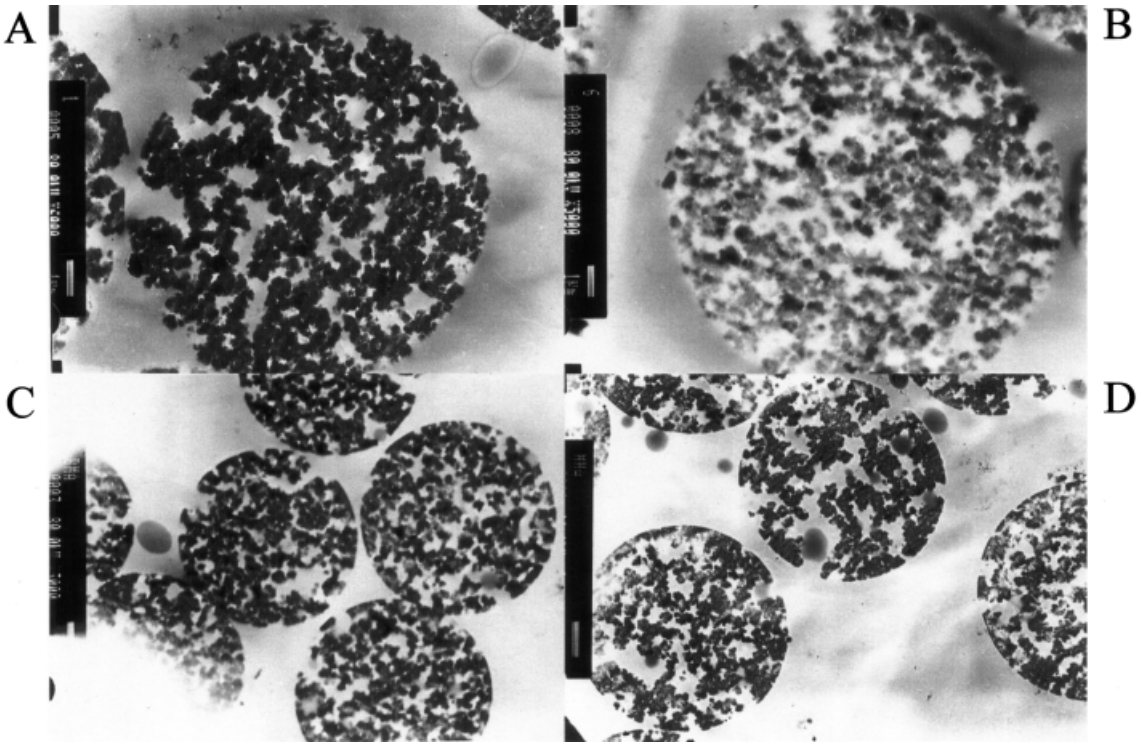

Figure 6 TEM photographs of OsO_4^{2-}-stained thin sections showing the internal structures of the macroporous particles produced in the presence of relatively hydrophobic monomers in the repolymerization stage: (A) poly(S–DVB) particles produced in the absence of PVA, (B) poly(S–DVB) particles produced in the presence of PVA, (C) poly(S–BMA–DVB) particles, and (D) poly(S–MMA–DVB) particles (the original magnifications were 6000× for A, 5000× for B, and 3000× for C and D).

in Figure 10. The strong carbonyl bands at 1740 cm^{-1} in the FTIR spectra of poly(S–MMA–DVB) and poly(S–BMA–DVB) particles showed the presence of the corresponding acrylic monomer in the bulk structure. For each particle type, the relative intensities of carbonyl bands in both FTIR and FTIR–DRS spectra were approximately the same. This indicated that concentrations of each acrylic monomer (i.e., BMA or MMA) in the particle interior and on the particle surface were approximately the same.

FTIR and FTIR–DRS spectra of uniform particles produced with relatively hydrophilic comonomers (i.e., EPMA, HEMA, and MAA) are given in Figure 11. The introduction of EPMA into the particle structure was confirmed by the strong carbonyl bands at 1740 cm^{-1} in both the FTIR and FTIR–DRS spectra of poly(S–EPMA–DVB) particles. The relative intensities of carbonyl bands (i.e., based on the intensities of aliphatic bands at 2900 cm^{-1}) appearing in both the FTIR and FTIR–DRS spectra of poly(S–EPMA–DVB) particles were very close. This indicated that bulk and surface concentrations of EPMA were roughly the same. In the FTIR spectrum of poly(S–EPMA–DVB) particles, a hydroxyl band with appreciable relative intensity was detected at 3500 cm^{-1}. This probably indicated that some part of EPMA introduced into the particle structure was hydrolyzed during the repolymerization step. However, the relative intensity of this band also showed that the hydrolyzed fraction of EPMA was not so significant. The relative intensity of the hydroxyl band (3500 cm^{-1}) in the FTIR–DRS spectrum of poly(S–EPMA–DVB) particles was not stronger than that observed in the FTIR–DRS spectrum of PVA-carrying poly(S–DVB) particles. This comparison supported that the hydroxyl band predominantly originated from EPMA chains hydrolyzed on the surface of poly(S–EPMA–DVB) particles.

The relative intensity of the hydroxyl band at 3500 cm^{-1} in the FTIR–DRS spectrum of poly(S–HEMA–DVB) particles was reasonably strong in comparison with that observed in the FTIR spectrum of the same particles. This indicated that

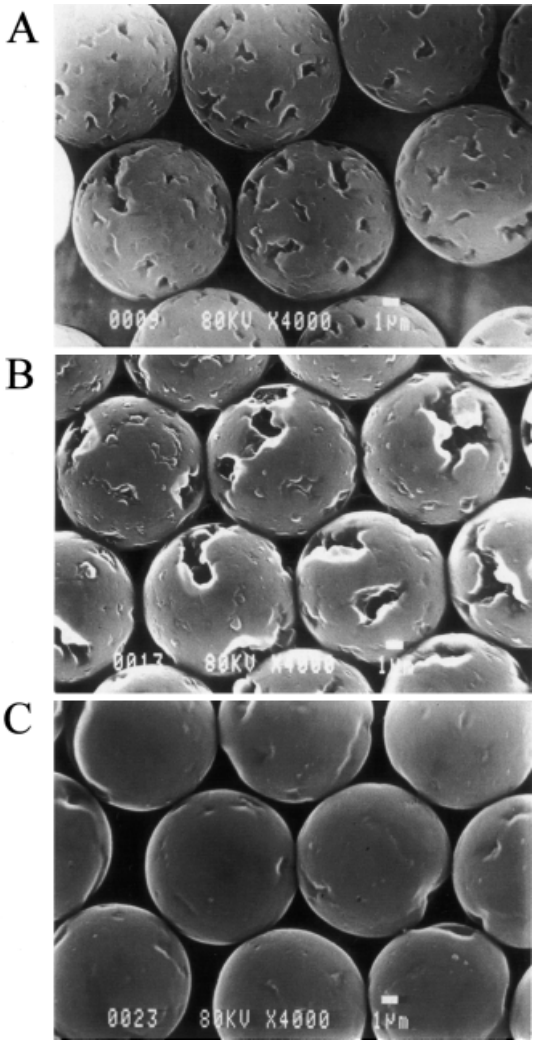

Figure 7 SEM photographs showing the detailed surface structures of the macroporous particles produced in the presence of relatively hydrophilic monomers in the repolymerization stage (for all photographs, the original magnification was 4000×): (A) poly(S–EPMA–DVB) particles, (B) poly(S–HEMA–DVB) particles, and (C) poly(S–MAA–DVB) particles.

the HEMA concentration was higher on the particle surface than in the particle interior. In FTIR and FTIR–DRS spectra of poly(S–MAA–DVB) particles, the strong and divided bands at 1740–1750 cm^{-1} probably originated from the carbonyl group of MAA. However, in the FTIR–DRS spectrum of poly(S–MAA–DVB) particles, the shoulder at 3500 cm^{-1} originating from the hydroxyl site of the carboxyl group was much stronger. This also indicated that the surface concentration of MAA was higher than that in the particle interior. Because HEMA and MAA are reasonably hydrophilic, these monomers were preferentially located on the surface of the corresponding particles produced in an aqueous emulsion medium. Highly porous forms of poly(S–MAA–DVB) and poly(S–HEMA–DVB) particles could also be achieved with some modifications to the seeded polymerization.[13]

A mechanism was proposed by Cheng et al.[8] for the pore formation process in large uniform latex

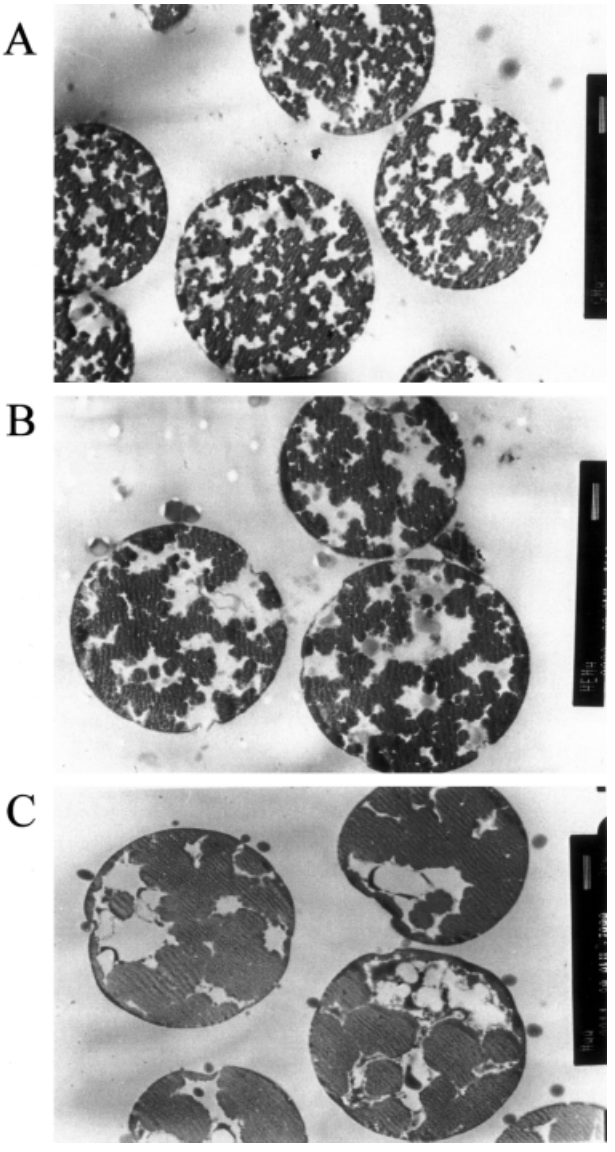

Figure 8 TEM photographs of OsO_4^{2-}-stained thin sections showing the internal structures of macroporous particles produced in the presence of relatively hydrophilic monomers in the repolymerization stage (for all photographs, the original magnification was 3000×): (A) poly(S–EPMA–DVB) particles, (B) poly(S–HEMA–DVB) particles, and (C) poly(S–MAA–DVB) particles.

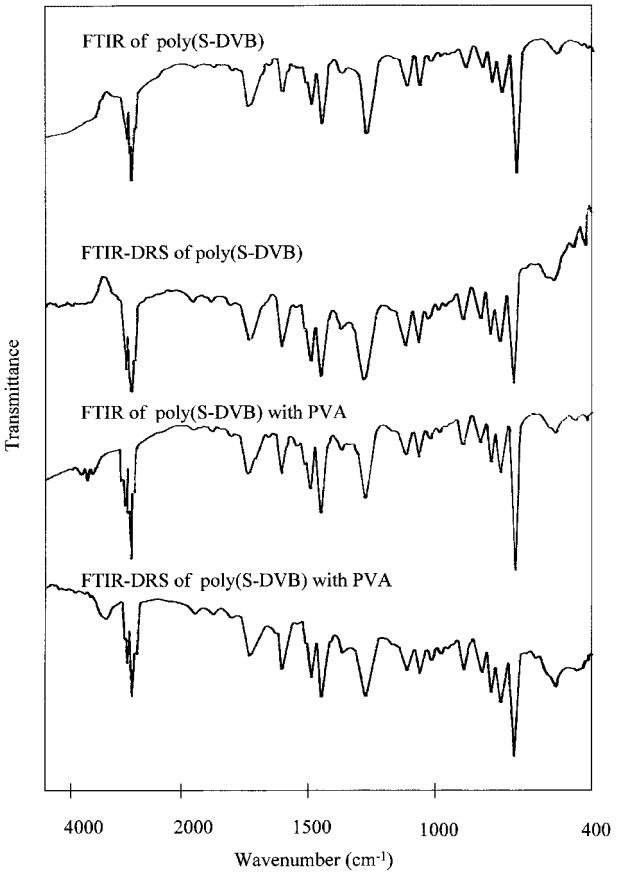

Figure 9 FTIR and FTIR–DRS spectra of plain poly(S–DVB) and poly(S–DVB) particles produced with PVA as the stabilizer in the repolymerization stage.

particles. According to this mechanism, the first stage in the pore formation process was described as the production and agglomeration of low-energy and highly crosslinked microspheres by phase separation taking place between the crosslinked polymer and the diluent phase, including linear PS and a nonsolvent. The fixation and binding of microspheres (i.e., agglomerate formation) occurred in the second stage, and the voids between the fixed microspheres filled with the linear polymer and nonsolvent.[8] By considering this mechanism and combining our results obtained with FTIR and electron microscopy, we make the following comments for the pore formation process in the presence of polar acrylic monomers.

There was a layer with reasonably low porosity or, in the nonporous form, on the surface of uniform particles obtained with relatively hydrophilic monomers (i.e., HEMA and MAA). FTIR–DRS results showed that these monomers were preferentially located in this layer. Then, an efficient phase separation probably did not occur in this region because of the high concentration of polar monomer. In other words, the crosslinked polymeric microspheres or aggregates, containing S and acrylic monomer, mixed well with the diluent phase on the particle surface.

Extremely large voids in the cross sections of poly(S–HEMA–DVB) and poly(S–MAA–DVB) can be explained by the formation of larger agglomerates during the pore formation process. These should occur by the adhesion and combination of smaller crosslinked gel microspheres in the forming particles. The adhesion and combination tendencies of these microspheres are probably higher for polar acrylic monomer. The rigid and stable gel microspheres, which are more resistant to adhesion and combination, should occur with the monomer mixtures containing only S and DVB (i.e., in the absence of a polar acrylic monomer). In such a case, the integrity of each microsphere is protected during the fixation process, and the

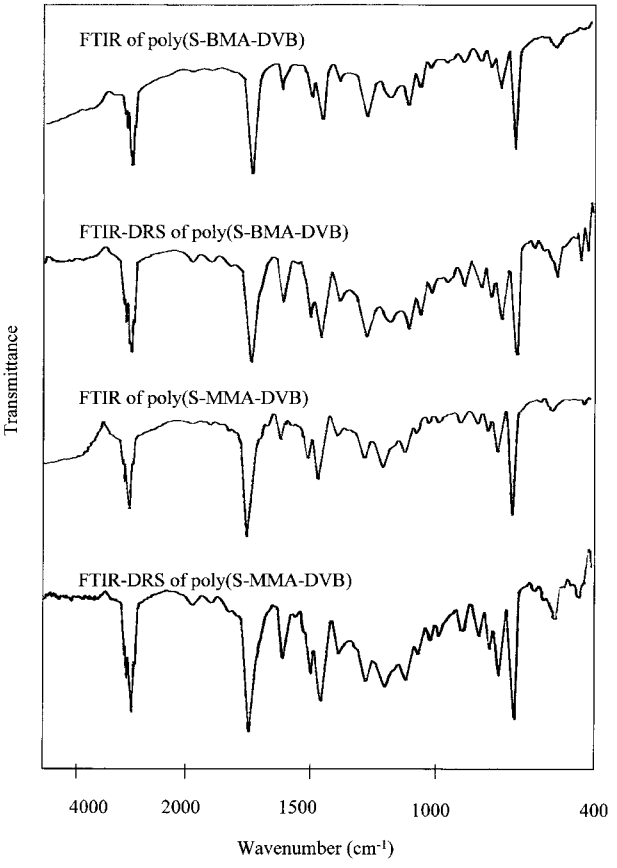

Figure 10 FTIR and FTIR–DRS spectra of poly(S–BMA–DVB) and poly(S–MMA–DVB) particles.

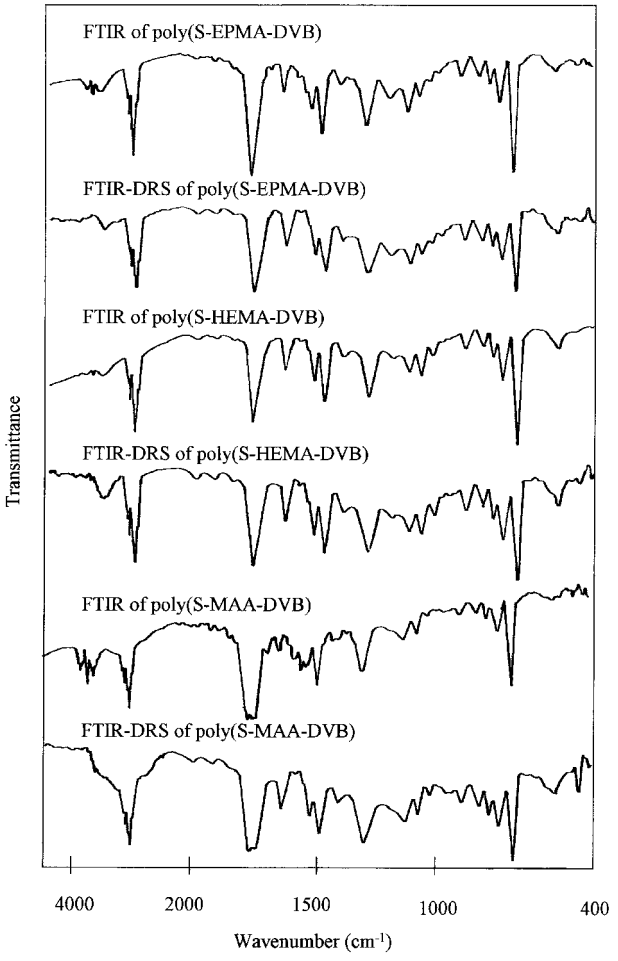

Figure 11 FTIR and FTIR–DRS spectra of poly(S–EPMA–DVB), poly(S–HEMA–DVB), and poly(S–MAA–DVB) particles.

individual microspheres do not mix or dissolve in each other. In this case, the voids, between the fixed individual microspheres filled with porogen, should be macropores of produced particles. The crosslinked microspheres occurring in the presence of a polar monomer probably have a stickier character. This property makes adhesion and combination easier. In a such a case, the integrity of individual microspheres cannot be protected, and large, continuos solid blocks are formed by combination, or excessive aggregation, of sticky microspheres during the fixation period. This case results in the formation of larger voids located between these blocks. However, the diluent absorption capacity of crosslinked microspheres generated during the pore formation process might be higher when a polar acrylic monomer is found in their structure. In this case, a larger amount of diluent is preferentially located in the swollen microspheres instead of being located in the voids between microspheres. The increasing diluent absorption capacity also may lead to a stickier form. Therefore, larger blocks are generated by the combination of these microspheres.

BSA Adsorption and Desorption Studies

Nonspecific protein adsorption behaviors of uniform, macroporous particles were investigated with BSA as the model protein. The amount of particles and the volume of the adsorption solution were fixed at 0.25 g and 40 mL, respectively. For the derivation of nonspecific BSA adsorption isotherms for each particle type, the BSA initial concentration was varied between 0.5 and 5.0 mg/mL. The adsorption experiments were performed at nearly the isoelectric point of BSA (pH 5) and at 25°C. For all particle types, the variation of the equilibrium BSA adsorption capacity with the initial BSA concentration is given in Figure 12. As seen here, the plateau value of the BSA adsorption capacity of particles decreased according to the following order: $Q_{P(S–DVB)} > Q_{P(S–EPMA–DVB)} > Q_{P(S–MMA–DVB)} > Q_{P(S–MAA–DVB)} > Q_{P(S–HEMA–DVB)} > Q_{P(S–BMA–DVB)} > Q_{PVA–P(S–DVB)}$. As defined in the literature, in the isoelectric point region, because the protein molecule was scarcely charged as a whole, BSA molecules were adsorbed onto the particles through nonelectrostatic forces.[21,48] In the case of plain poly(S–DVB) particles with the most hydrophobic surface, hydrophobic interaction is probably the predominant driving force to nonspecific BSA adsorption at the isoelectric point.[48] For this reason, the highest BSA adsorption capacity was obtained with plain poly(S–DVB) particles.

Nonspecific BSA adsorption capacities of poly(S–EPMA–DVB) particles were approximately equal to those of plain poly(S–DVB). The mechanism of BSA adsorption onto poly(S–EPMA–DVB) particles is probably different than for the others. Although a physical adsorption process is valid for all particle types tried in this study, BSA adsorption onto poly(S–EPMA–DVB) particles probably occurs by either physical interaction or covalent-bond formation. The epoxypropyl group of EPMA has a direct reaction ability with the amino groups of BSA under the selected adsorption conditions. The proposed reaction scheme is given in Figure 13. Therefore, the dominant mechanism for BSA binding onto the poly(S–EPMA–DVB) particles is probably a chemical adsorption process. The high BSA adsorption capac-

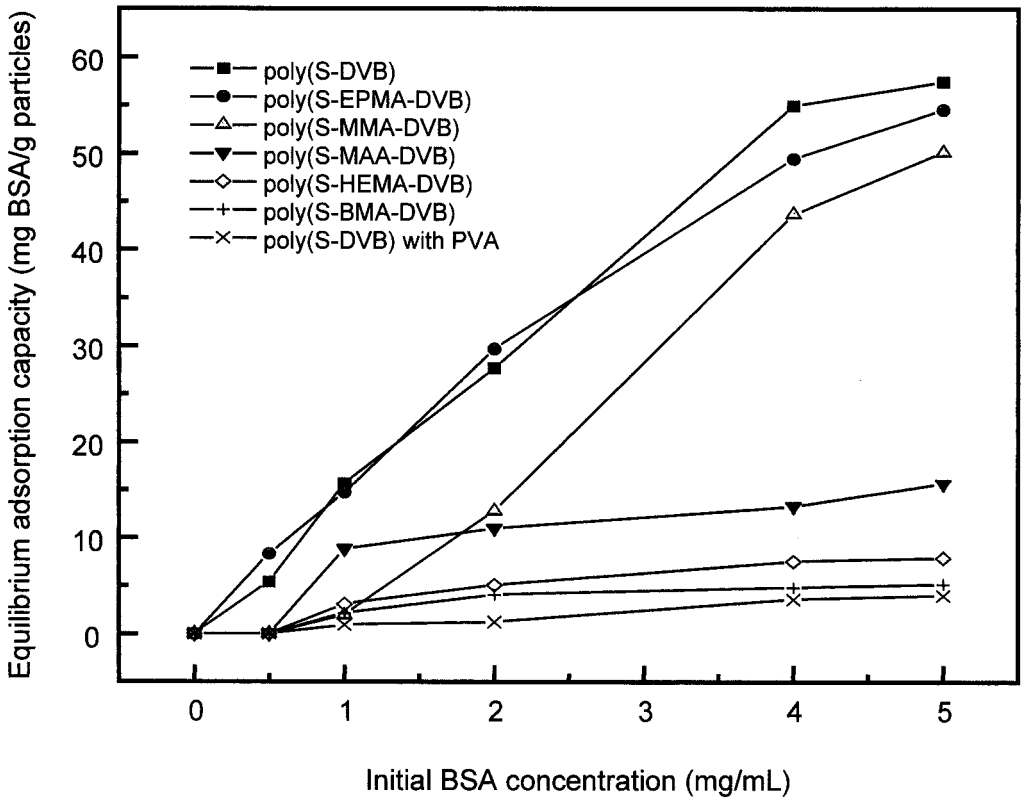

Figure 12 Variation of the equilibrium BSA adsorption capacity of the macroporous particles with the initial BSA concentration.

ity of these particles should be explained by the covalent binding of BSA molecules onto the particle surface.

The maximum nonspecific BSA adsorption capacity of poly(S–MMA–DVB) particles was lower than that of plain poly(S–DVB). The use of MMA in the repolymerization step probably led to a more hydrophilic particle surface relative to that of plain poly(S–DVB). Therefore, the introduction of MMA probably reduced the hydrophobic inter-

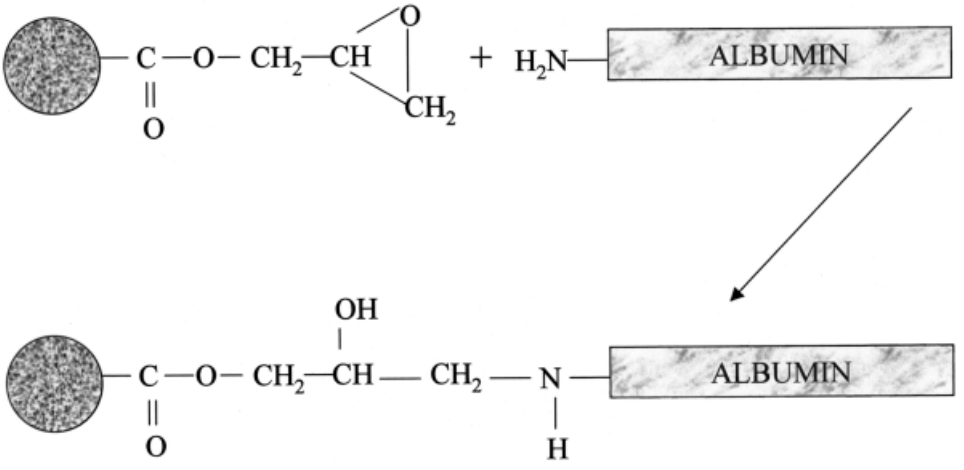

Figure 13 Proposed reaction scheme for the covalent binding of BSA molecules onto the epoxypropyl groups of poly(S–EPMA–DVB) particles.

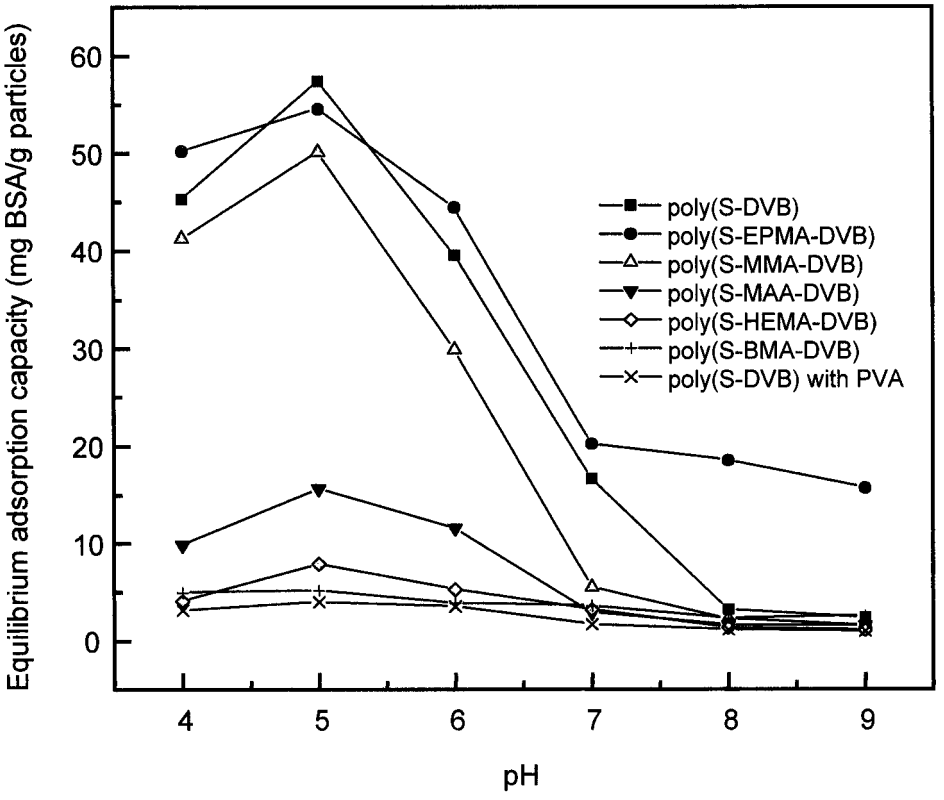

Figure 14 Effect of pH on the equilibrium BSA adsorption capacity of the macroporous particles.

action between BSA and the particle surface, and lower BSA adsorption was obtained. Okubo et al.[23] investigated the nonspecific BSA adsorption behaviors of submicrometer PS and poly(MMA) latices produced by a conventional emulsion polymerization procedure. They found that the nonspecific albumin adsorption capacity of poly(MMA) latex was lower than that of PS.

The results in Figure 12 indicate that relatively lower BSA adsorption capacities were obtained with uniform particles functionalized with acrylic monomers having polar hydrophilic groups (i.e., MAA and HEMA). A comparison of FTIR and FTIR–DRS spectra of the particles produced in the presence of HEMA or MAA clearly showed that the concentration of HEMA or MAA on the corresponding particle surfaces was higher than its bulk concentration. For these particles, a hydrous poly(HEMA)-rich or poly(MAA)-rich layer on the particle surface probably led to weak hydrophobic interaction between the particles and BSA. In the literature, significantly lower nonspecific BSA adsorption capacities, relative to that of plain PS latex, have also been reported for poly(S–HEMA) particles produced by conventional emulsion polymerization in the submicrometer range.[20,23] In our results, the higher adsorption capacity of MAA-functionalized particles, relative to that of HEMA-carrying ones, is probably explained by the hydrogen-bond formation between BSA and carboxyl groups of the MAA-rich surface layer.[22,49]

PVA-carrying latex particles provided the lowest equilibrium BSA adsorption capacities at all BSA concentrations. PVA is one hydrophilic agent widely used for reducing nonspecific protein adsorption onto hydrophobic polymeric materials.[26] Although BMA was one of the most hydrophobic comonomers among those tried, BSA adsorption capacities obtained with the BMA-carrying particles were surprisingly low. This result did not obey the tendency expected from the hydrophilicity of the acrylic monomers.

The effect of pH on the BSA adsorption capacity of the uniform, macroporous particles is given in Figure 14. These experiments were performed at 25°C with an initial BSA concentration of 5 mg/mL. As seen here, no significant nonspecific

Table III Desorption Ratios Achieved with the Macroporous Particles Loaded with Different BSA Initial Concentrations

Particle Type	Equilibrium BSA Adsorption Capacity (mg of BSA/g of particle)	Desorption Ratio (wt % adsorbed BSA)
Plain poly(S–DVB)	57.4	83.4
Poly(S–DVB) with PVA	3.9	96.2
Poly(S–BMA–DVB)	5.2	92.1
Poly(S–MMA–DVB)	50.1	85.7
Poly(S–EPMA–DVB)	54.5	5.9
Poly(S–HEMA–DVB)	7.9	80.9
Poly(S–MAA–DVB)	15.6	89.8

BSA adsorption onto the poly(S–DVB) particles, produced in the presence of PVA, was observed at all pH values. As expected, maximum equilibrium adsorption capacity was obtained at the isoelectric point of BSA (pH 5.0) for all other particles. The maximum albumin adsorption observed at pH 5 is probably explained by the minimum water solubility of albumin at the isoelectric point. Note that similar behavior was observed for PS, poly(S–HEMA), and poly(S–acrylamide) copolymer latices of submicrometer size.[20,21,48] The equilibrium adsorption capacity markedly decreased in the pH region higher than the isoelectric point (pH $>$ 5). Note that all types of latex particles produced in this study possessed negatively charged surfaces (Table II). As stated in the literature, electrostatic repulsion acts between negatively charged latex particles and albumin at pH values higher than the isoelectric point.[21,48] In physical adsorption, electrostatic repulsion is probably the main reason for the decrease in the adsorption capacity. Although very low (i.e., nearly zero) equilibrium adsorption capacities were obtained with all particles in the alkaline pHs (i.e., 8 and 9), poly(S–EPMA–DVB) particles exhibited an appreciable BSA adsorption in this range. This behavior probably originated from the BSA adsorption mechanism, which was valid for EPMA-carrying particles (i.e., adsorption via covalent-bond formation). However, the decrease observed in the albumin adsorption capacity of poly(S–EPMA–DVB) particles probably indicated that chemical interaction between the amine groups of BSA and epoxypropyl groups was not so strong in the alkaline pH region.

The desorption of BSA adsorbed from the uniform particles was studied in batch fashion. The desorption ratio was defined as the ratio of the amount of BSA released in the desorption medium to the amount of BSA adsorbed onto the particles. The desorption ratios, achieved with particles loaded with an initial BSA concentration of 5 mg/mL, are presented in Table III. Except for poly(S–EPMA–DVB), approximately 80–90% of the adsorbed BSA could be desorbed from the surfaces of all particles. In other words, the macroporous particles, except for poly(S–EPMA–DVB), exhibited reversible BSA adsorption–desorption behavior. However, the desorption ratio observed with poly(S–EPMA–DVB) particles was very low (ca. 5% w/w). This indicated that most BSA was adsorbed irreversibly onto poly(S–EPMA–DVB) particles. The validity of a chemical adsorption mechanism for poly(S–EPMA–DVB) particles (i.e., covalent binding of BSA molecules onto the surface of EPMA-carrying particles) was confirmed by this result.

CONCLUSIONS

As chromatographic support materials in GPC applications, uniform, macroporous particles approximately 10 μm in size were prepared with different surface chemistries by the inclusion of different acrylic monomers in a multistage microsuspension polymerization. The presence of acrylic monomer strongly affected the surface and bulk morphology of the final particles. Although highly porous particles could be achieved with relatively hydrophobic monomers such as S, BMA, MMA, and EPMA, the use of hydrophilic monomers such as HEMA and MAA led to particles with lower porosity. Because the nonspecific interactions between the proteins and stationary phase materials are important in GPC applications, the adsorption of albumin onto the particles obtained with different surface chemistries was

investigated. The particles with relatively hydrophobic character [i.e., plain poly(S–DVB), poly(S–MMA–DVB), and poly(S–EPMA–DVB)] provided high nonspecific albumin adsorption. Lower albumin adsorption was observed with the particles produced in the presence of hydrophilic acrylic monomers such as MAA and HEMA. Poly(S–DVB) particles functionalized with PVA gave nearly zero albumin adsorption.

REFERENCES

1. Svec, F.; Frechet, J. M. J. Science 1996, 273, 205.
2. Ellingsen, T.; Aune, O.; Ugelstad, J.; Hagen, S. J Chromatogr 1990, 535, 147.
3. Wang, Q. C.; Svec, F.; Frechet, J. M. J. J Polym Sci Part A: Polym Chem 1994, 32, 2577.
4. Galia, M.; Svec, F.; Frechet, J. M. J. J Polym Sci Part A: Polym Chem 1994, 32, 216.
5. Ugelstad, J.; Kaggerad, K. H.; Hansen, K.; Berge, A. Makromol Chem 1979, 180, 737.
6. Ugelstad, J. Makromol Chem 1978, 179, 815.
7. Cheng, C. M.; Micale, F. J.; Vanderhoff, J. W.; El-Aasser, M. S. J Polym Sci Part A: Polym Chem 1992, 30, 235.
8. Cheng, C. M.; Vanderhoff, J. W.; El-Aasser, M. S. J Polym Sci Part A: Polym Chem 1992, 30, 245.
9. Smigol, V.; Svec, F.; Hosoya, K.; Wang, Q.; Frechet, J. M. J. Angew Makromol Chem 1992, 195, 151.
10. Tuncel, A.; Tuncel, M.; Salih, B. J Appl Polym Sci 1999, 71, 2271.
11. Tuncel, A. J Appl Polym Sci 1999, 71, 2291.
12. Çamlı, T.; Şenel, S.; Tuncel, A. J Biomater Sci Polym Ed 1999, 10, 875.
13. Tuncel, A.; Tuncel, M.; Alagöz, C.; Bahar, T.; Ergun, B. Colloids Surf A 2002, 197, 79.
14. Okubo, M.; Nakagawa, T. Colloid Polym Sci 1992, 270, 853.
15. Omi, S.; Katami, K.; Yamamoto, A.; Iso, M. J Appl Polym Sci 1994, 51, 1.
16. Omi, S.; Katami, K.; Taguchi, T.; Kaneko, K.; Iso, M. J Appl Polym Sci 1995, 57, 1013.
17. Omi, S. Colloids Surf A 1996, 109, 97.
18. Tamai, H.; Hasegawa, M.; Suzawa, T. J Appl Polym Sci 1989, 38, 406.
19. Suzawa, T.; Shirahama, H.; Fujimoto, T. J Colloid Interface Sci 1982, 86, 144.
20. Shirahama, H.; Suzawa, T. J Colloid Interface Sci 1985, 104, 416.
21. Shirahama, H.; Shikawa, T.; Suzawa, T. Colloid Polym Sci 1989, 267, 587.
22. Tamai, H.; Hasegawa, M.; Suzawa, T. Colloids Surf 1989, 40, 63.
23. Okubo, M.; Azume, I.; Yamamoto, Y. Colloid Polym Sci 1990, 268, 598.
24. Shirahama, H.; Lyklema, J.; Norde, W. J Colloid Interface Sci 1990, 139, 177.
25. Tuncel, A.; Denizli, A.; Olcay, M.; Abdelaziz, M.; Pişkin, E. Clin Mater 1992, 11, 139.
26. Tuncel, A.; Denizli, A.; Purvis, D.; Lowe, C. R.; Pişkin, E. J Chromatogr 1993, 634, 161.
27. Tuncel, A. Colloid Polym Sci 2000, 278, 1126.
28. Tuncel, A.; Kahraman, R.; Pişkin, E. J Appl Polym Sci 1993, 50, 303.
29. Tuncel, A.; Kahraman, R.; Pişkin, E. J Appl Polym Sci 1994, 51, 1485.
30. Ayhan, H.; Tuncel, A.; Bor, N.; Piskin, E. J Biomater Sci Polym Ed 1995, 7, 329.
31. Bulmuş, V.; Tuncel, A.; Pişkin, E. J Appl Polym Sci 1996, 60, 697.
32. Takahashi, K.; Miyamori, S.; Uyama, H.; Kobayashi, S. J Polym Sci Part A: Polym Chem 1996, 34, 175.
33. Horak, D. J Polym Sci Part A: Polym Chem 1999, 37, 3785.
34. Tuncel, A. Polymer 2000, 41, 1257.
35. Tuncel, A.; Serpen, E. Colloid Polym Sci 2001, 279, 240.
36. Kawaguchi, H.; Fujimoto, K.; Mizuhara, Y. Colloid Polym Sci 1992, 270, 53.
37. Okubo, M.; Ahmad, H. Colloid Polym Sci 1996, 274, 112.
38. Sugiyama, K.; Mitsuno, S.; Shiraishi, K. J Polym Sci Part A: Polym Chem 1997, 35, 3349.
39. Kondo, A.; Imura, K.; Nakama, K.; Higahistani, K. J Ferment Bioeng 1994, 78, 241.
40. Sun, Y. M.; Yu, C. W.; Liang, H. C.; Chen, J. P. J Dispersion Sci Technol 1999, 20, 907.
41. Elmas, B.; Çamlı, T.; Tuncel, M.; Şenel, S.; Tuncel, A. J Biomater Sci Polym Ed 2001, 12, 283.
42. Delair, T.; Meunier, F.; Elaissari, A.; Charles, M. H.; Pichot, C. Colloids Surf A 1999, 153, 341.
43. Elaissari, A.; Chevalier, Y.; Ganachaud, F.; Delair, T.; Pichot, C. Langmuir 2000, 16, 1261.
44. Götting, N.; Fritz, H.; Maier, M.; Stamm, J. V.; Schoofs, T.; Bayer, E. Colloid Polym Sci 1999, 277, 145.
45. Delair, T.; Pichot, C.; Madrand, B. Colloid Polym Sci 1994, 272, 72.
46. Sauzedde, F.; Elaissari, A.; Pichot, C. Macromol Symp 2000, 151, 617.
47. Handbook of Chemistry and Physics, 55th ed.; Weast, R. C., Ed.; CRC: Cleveland, OH, 1974.
48. Shirahama, H.; Takeda, K.; Suzawa, T. J Colloid Interface Sci 1986, 109, 552.
49. Shirahama, H.; Suzawa, T. Colloid Polym Sci 1985, 263, 141.